6.10.3 Symptoms of Oil Whirl and Oil Whip

1) The frequency spectrum contains a sub-synchronous frequency component at between 42 - 48% of running speed. In the instantaneous frequency domain this sub-synchronous component tends to be unstable. Figure 6.24 clearly illustrates the sub-synchronous components of 42,5 Hz and 43,5 Hz which is 45,9% and 47% respectively of the running speed of 92,5 Hz.

2) Since oil whirl tracks a fairly constant ratio of rotative speed, this will show up as a sub-synchronous component over a certain speed range on the waterfall plot. Figure 6.25, a waterfall plot indicates that oil whirl is occurring between 5500 RPM and 7000 RPM. (See top left hand side of plot).

3) Another simple way of observing oil whirl is to examine the orbits from two proximity probes on an oscilloscope. Shaft orbits for different synchronous and half synchronous whirl components were simulated using a computer programme which generated these plots, as shown in Figure 6.26. The smaller orbit due to the sub-synchronous whirl component will tend to rotate inside the bigger orbit when viewed on an oscilloscope, as shown below in Figure 6.27.

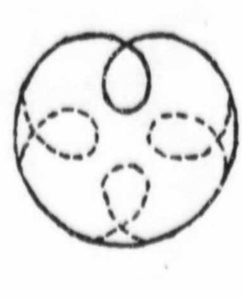

FIGURE 6.27

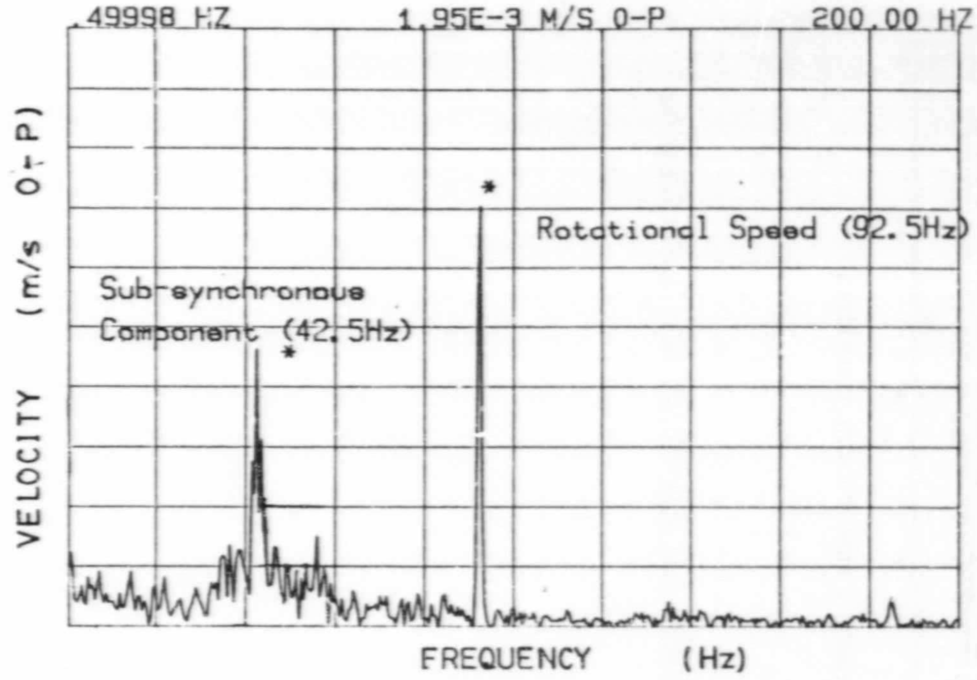

M/S 0-P	HERTZ
904.E-6	42.502
612.E-6	43.502
567.E-6	46.002
576.E-6	50.002
1.37E-3	92.504

SUB-SYNCHRONOUS WHIRL COMPONENT SPECTRUM

FIGURE 6.24

ESCOM
MECHANICAL T&R
DYNAMICS & NOISE

RUNDOWN

RUN: 1

PLANT ID: DYNAMICS LABORATORY
TRAIN ID: ROTOR TEST KIT
MACHINE ID: NDE BEARING
PROBE ID: HORIZONTAL

DATE: 09 OCT 85

PLOT NO:

TIME: [illegible]:28

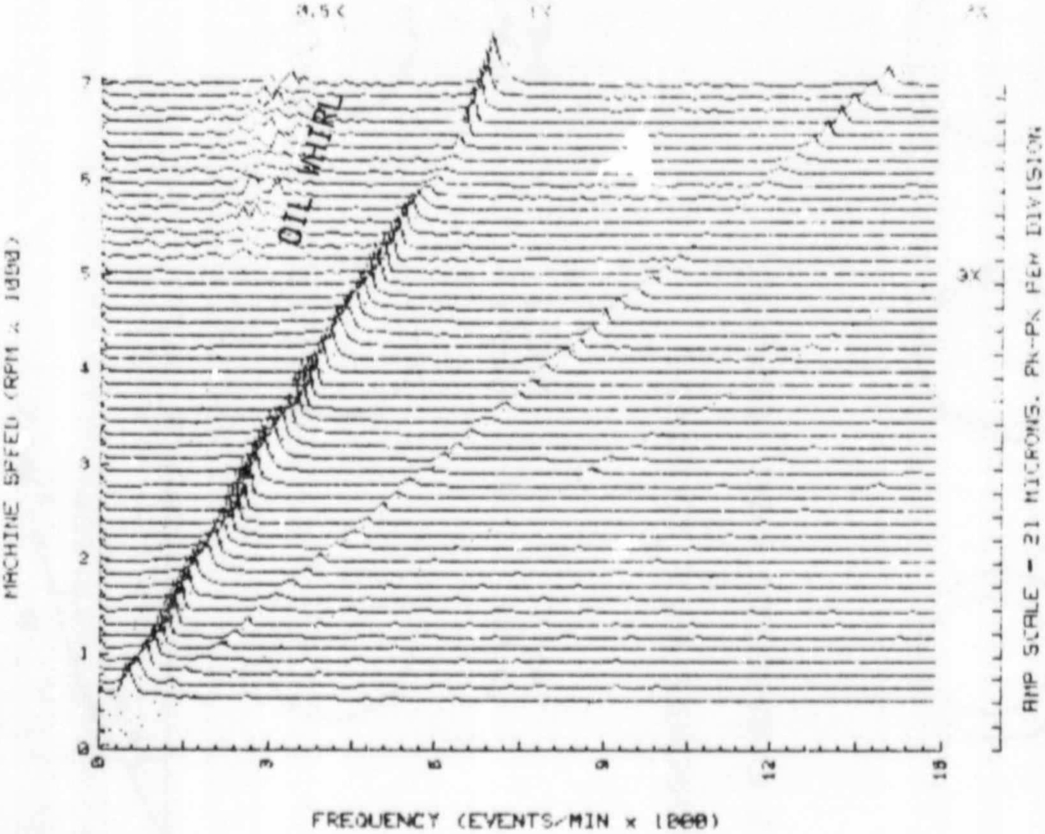

<u>CASCADE PLOT ILLUSTRATING OIL WHIRL</u>

FIGURE 6.25

ESCOM
MECHANICAL
DYNAMICS & NOISE

PLOT NO:

PLANT ID: DYNAMICS LABORATORY
TRAIN ID: ROTOR TEST KIT
MACHINE ID: NDE BEARING
RUNDOWN
PROBE ID: HORIZONTAL

RUN: 1
DATE: 09 OCT 85
TIME: 11:28

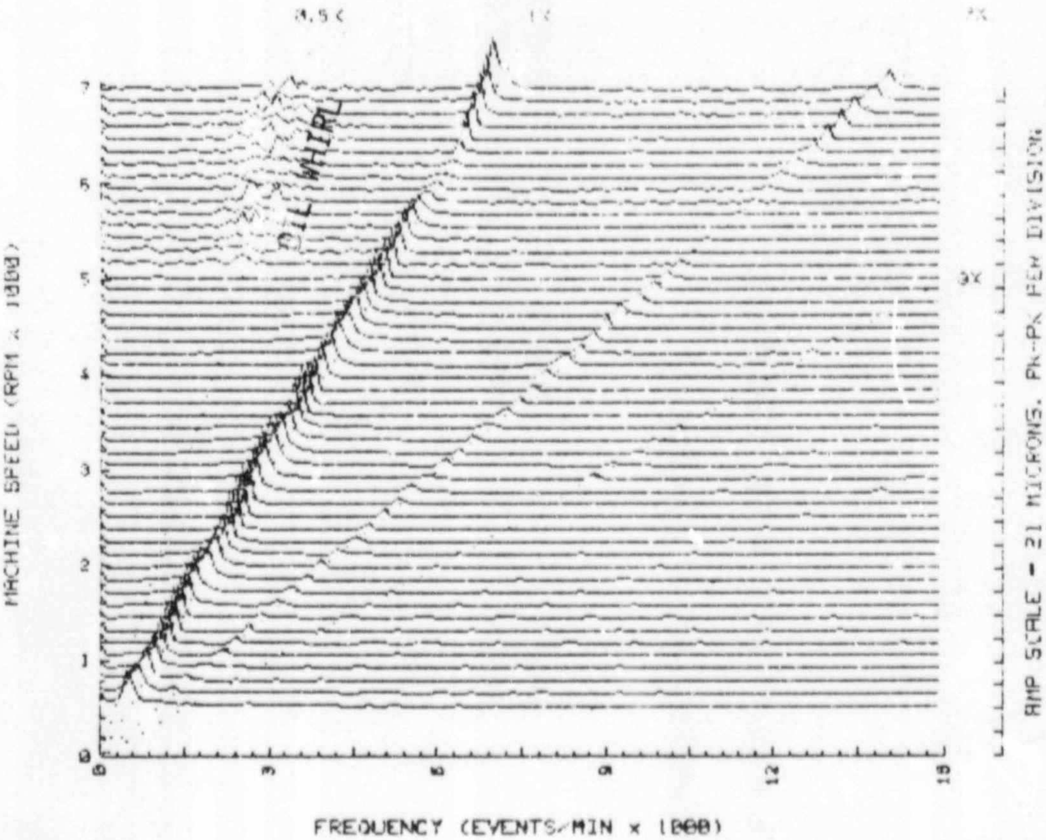

CASCADE PLOT ILLUSTRATING OIL WHIRL

FIGURE 6.25

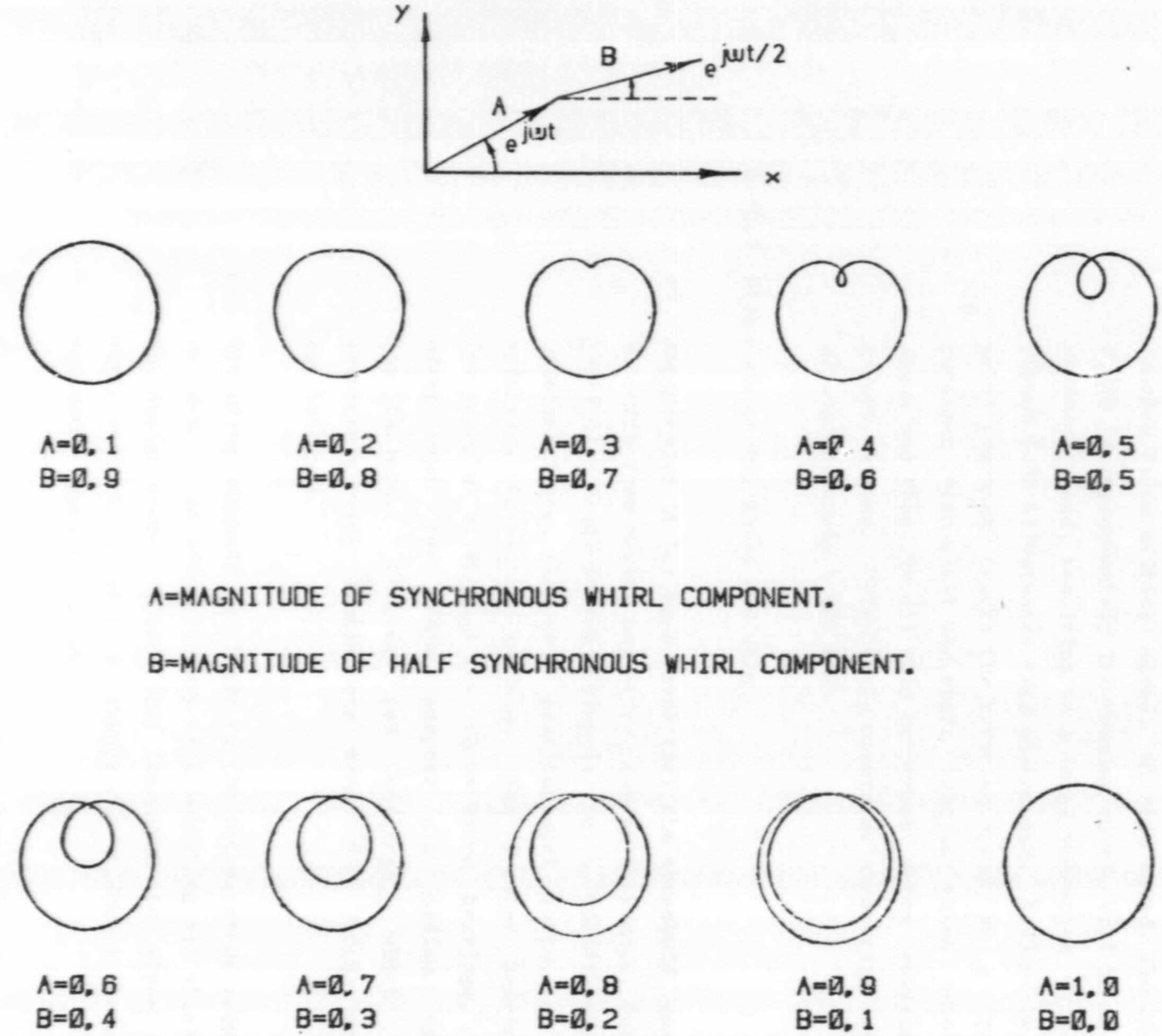

SHAFT ORBITS WITH VARYING SYNCHRONOUS AND SUB SYNCHRONOUS WHIRL COMPONENTS.

FIGURE 6.26

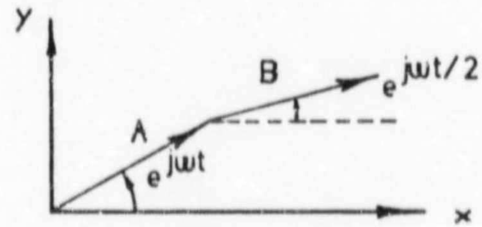

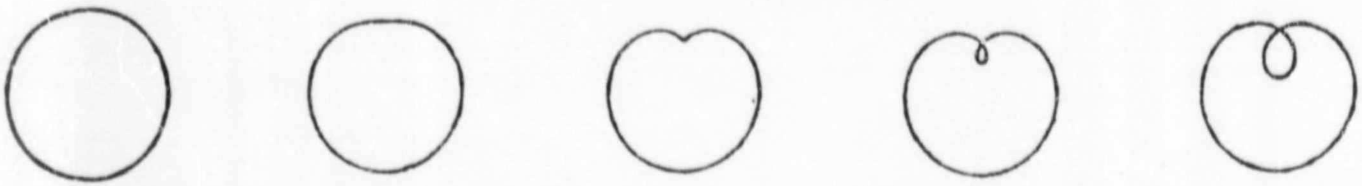

A=0.1 B=0.9	A=0.2 B=0.8	A=0.3 B=0.7	A=0.4 B=0.6	A=0.5 B=0.5

A=MAGNITUDE OF SYNCHRONOUS WHIRL COMPONENT.

B=MAGNITUDE OF HALF SYNCHRONOUS WHIRL COMPONENT.

A=0.6 B=0.4	A=0.7 B=0.3	A=0.8 B=0.2	A=0.9 B=0.1	A=1.0 B=0.0

SHAFT ORBITS WITH VARYING SYNCHRONOUS AND SUB SYNCHRONOUS WHIRL COMPONENTS.

FIGURE 6.26

4) Oil whirl may also cause instability when the shaft reaches twice critical speed. At this speed, the whirl, which is approximately 1/2 running speed, will be at the critical speed, resulting in a large vibration response Figure 6.28 illustrates this phenomenon. Notice the oil whirl component tracks the rotative speed at a fairly constant ratio until the shaft reaches twice critical speed and then the oil whip component moves vertically across the map. This change occurs at a rotative speed of approximately 4 900 RPM

6.10.4 Diagnosis of Oil Whirl and Whip

1) Empirically it has been found that the threshold speed, at which free motion may arise, can be increased for a particular rotor by subjecting it to a unidirectional constant force, such as a gravitational force, or by modifying the bearing profile. Non-circular bearings, for example elliptical or three-lobed bearings, are often used for this purpose in medium speed applications. Tilting pad bearings, which are inherently very stable are used for high speed applications.

2) Providing adequate stiffness to the rotor, rotor support or both, is an effective way of eliminating oil whirl at the design stage. A practical approach to alter the shaft critical speed is to change the distance between the rotor support bearings.

3) Changes in oil viscosity or pressure can also reduce oil whirl.

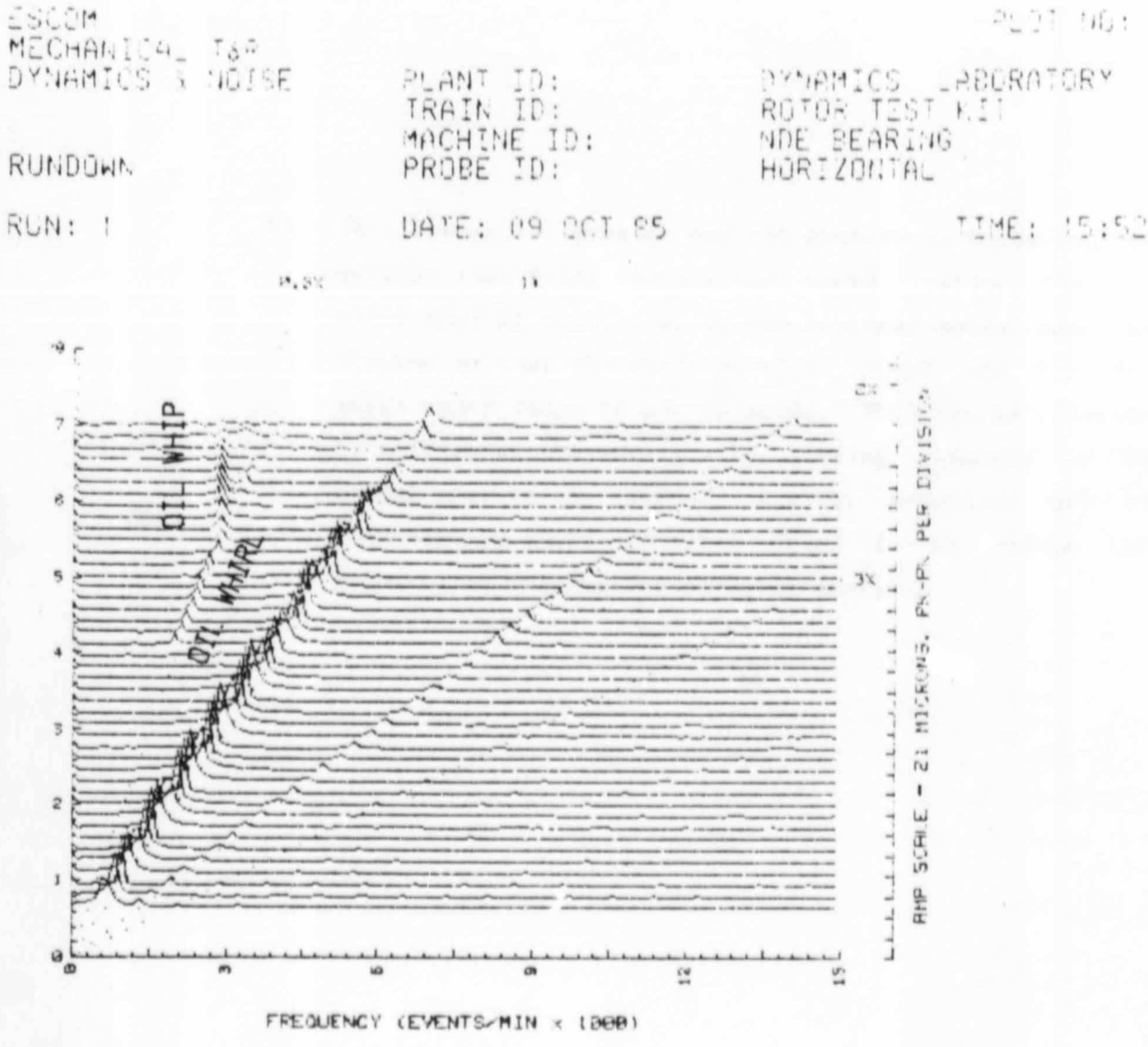

CASCADE PLOT ILLUSTRATING OIL WHIRL AND OIL WHIP

FIGURE 6.28

4) If oil whirl is present and the machine is to be run at greater than twice the critical speed, either the oil whirl must be suppressed or the critical speed must be altered so that the shaft critical speed and the oil whirl speed range do not coincide. This can be achieved by stiffening the rotor, the bearing supports or by adding mass to the rotor. Another practical way of changing the shaft critical speed is to change the geometry of the bearing pedestal centres.

6.11 SHAFT CENTRE LINE POSITION ANALYSIS

6.11.1 Introduction

Shaft centre line position is a graphical presentation which tracks the location of the shaft centre line with respect to the geometric centre of a bearing. This presentation also permits computation of the attitude angle of the shaft with the bearing. A typical shaft centre line plot that was generated using the Bently Nevada rotor kit can be seen in Figure 6.29. Each bearing type, plain sleeve, multi-lobe tilting pad etc, has a design or normal range of values of attitude angle. If the observed attitude angle is significantly different from the norm, it usually indicates that some external preload is forcing it to an abnormal position. The stability of a machine is directly related to the operating attitude angle.

6.11.2 Measurement of Shaft Centre Line Position

The data necessary for the graphical representation of the shaft centre line is obtained using the DC voltage from two proximity probes (located 90° apart in the vertical plane), at fixed increments of speed during the run-up or coastdown of a machine. The DC voltages and the corresponding speeds from the rotor kit can be seen in the table on the right hand side of Figure 6.29.

ESCOM DYNAMICS & NOISE

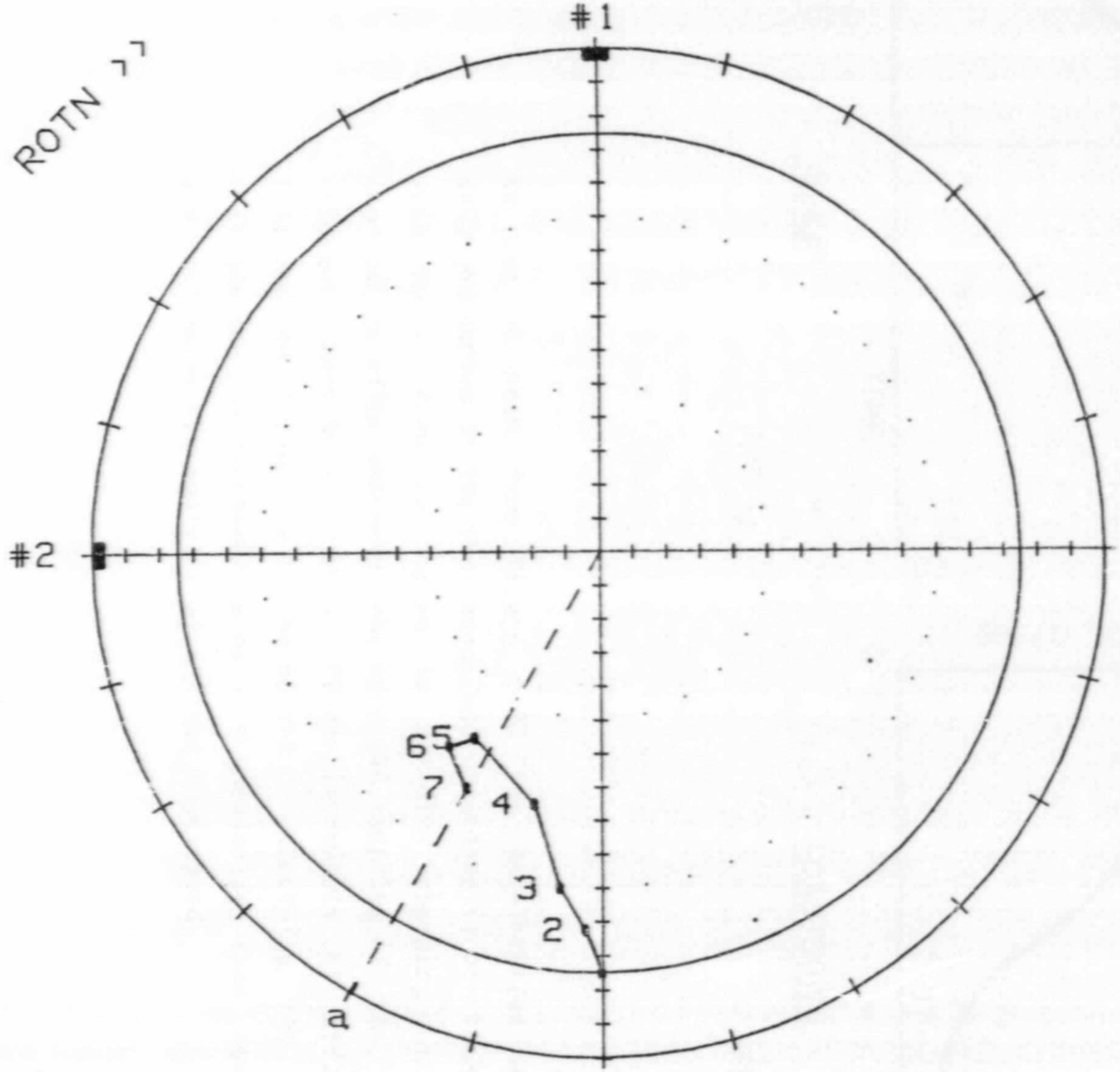

PLANT ID:	DYNAMICS LAB
TRAIN ID:	ROTOR TEST KIT
MACHINE ID:	NDE BEARING
PROBE #1 ID:	VERTICAL
PROBE #2 ID:	HORIZONTAL
RUN	1
DATE	23 OCT 84
TIME	10 h00

#	RPM	TIME	DC VALUES (Volts) PROBE #1	PROBE #2
1	0		-4.00	-4.00
2	1000		-3.95	-3.98
3	2000		-3.90	-3.95
4	3000		-3.80	-3.92
5	5000		-3.72	-3.85
6	6000		-3.73	-3.82
7	7000		-3.78	-3.84

#	REMARKS
1	ZERO SPEED

SHAFT CENTERLINE PLOT

ATTITUDE ANGLE (a) = 30 DEG
BEARING CLEARANCE = 250 MICRONS

PLOT RADIUS =150 MICRONS/ .60 VOLTS PROBE #1 SF = 4 mV/MICRON
TIC SPACING = 10 MICRONS PROBE #2 SF = 4 mV/MICRON
SHAFT MOVEMENT VECTOR = 68 MICRONS @ 126 DEG

FIGURE 6.29

If the speed of a machine cannot be controlled a problem could arise in acquiring the DC voltages. A plot of speed versus time for a normal uncontrolled run-up and coastdown of a typical machine is shown in Figure 6.30 below.

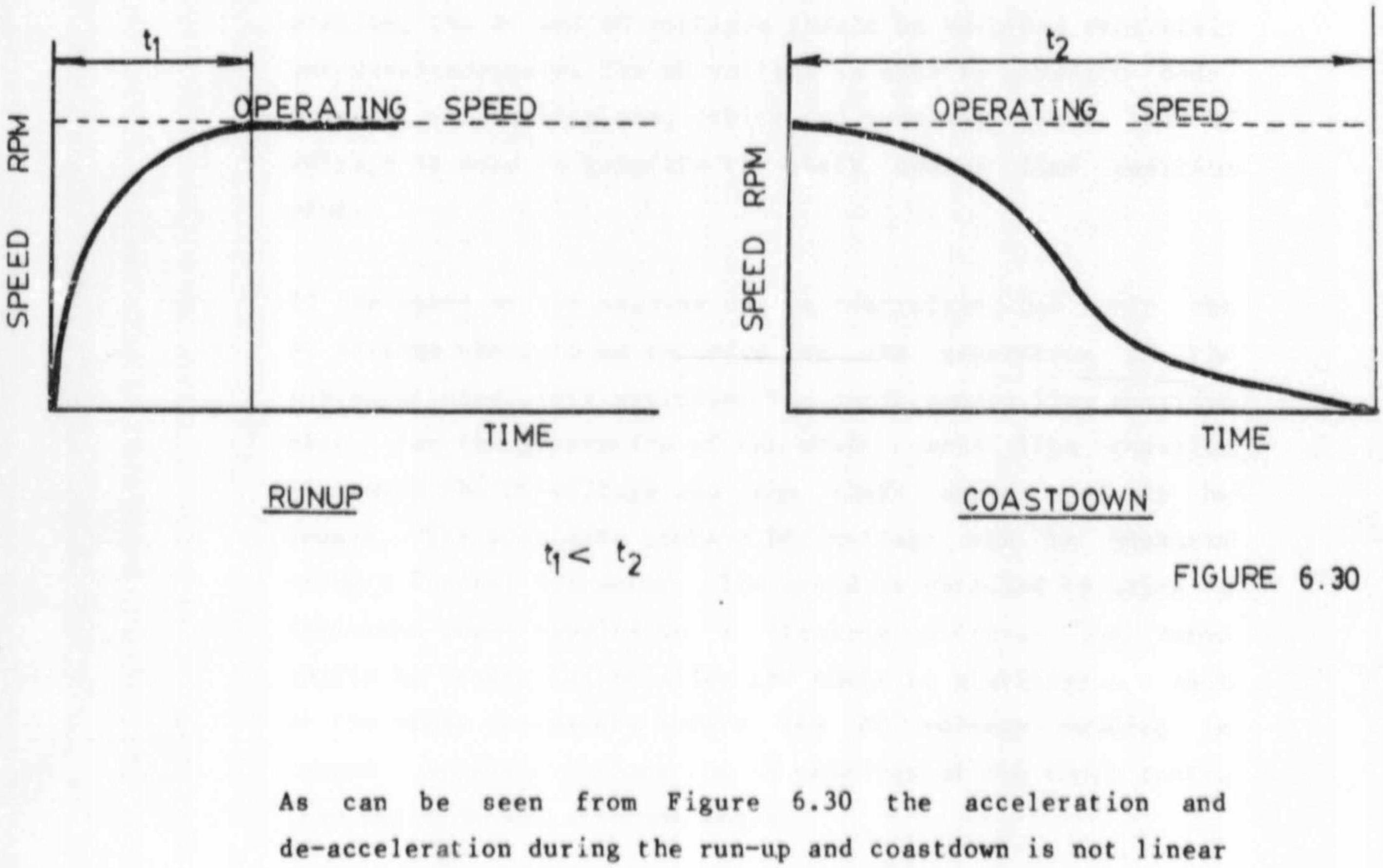

FIGURE 6.30

As can be seen from Figure 6.30 the acceleration and de-acceleration during the run-up and coastdown is not linear with time. When the speed is rapidly changing e.g. immediately after shutdown, the required sampling of the DC voltages cannot be achieved at fixed increments of speed. This problem of sampling can be solved by recording the DC voltages and the keyphasor pulse at a particular tape speed and performing the analysis at a lower tape speed.

Another problem associated with the recording of AC and DC voltages is that of signal to noise ratio. The DC voltage is normally of the order of 8 VDC while the AC voltage ranges from 1 mV to 500 mV. If the DC and AC voltages are simultaneously recorded, the DC voltage has to be attenuated so as not to overload amplifiers on the tape recorder. In the process the AC signal is also attenuated resulting in a decrease in the signal to noise ratio. To solve this problem, the DC and AC voltages should be recorded separately but simultaneously. The AC voltage is used to generate Bode, Nyquist, waterfall plots, orbits and spectra, while the DC voltage is used to generate the shaft centre line position plot.

If the speed of the machine can be controlled then only the AC voltage needs to be recorded for the generation of the abovementioned plots excluding the shaft centre line position plot. For the generation of the shaft centre line position plot only the DC voltage and the shaft speed need to be logged. The proximity probe's DC voltage can be measured using a Digital Voltmeter. The speed is obtained by using a keyphasor probe coupled to a tracking filter. The speed should be controlled to allow the shaft to stabilise at each of the speed increments before the DC voltage reading is logged. Appendix 3 shows the calculation of the shaft centre line position and attitude angle.

Not only can the shaft centre line position be plotted during a run-up or coastdown, but the attitude angle and the shaft movement vector can be trended as seen in Figure 6.31. Transient data of the shaft centre line position at various speed increments during a run-up is stored. This is depicted from point A to point B in Figure 6.31. The shaft centre

SHAFT CENTRELINE MOVEMENT

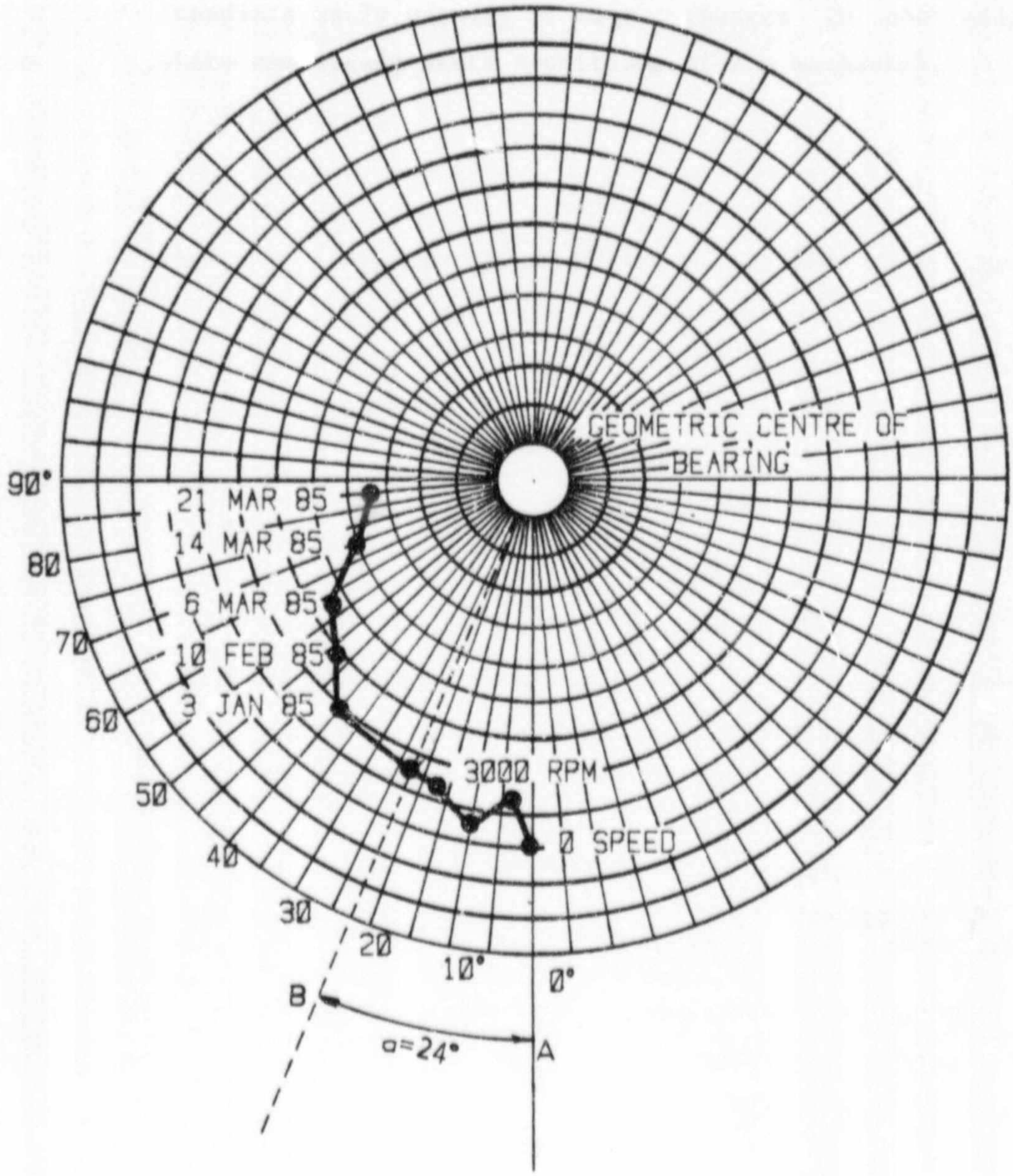

FIGURE 6.31

line position is subsequently taken monthly at the operating speed of the machine (3000 RPM), for trending purposes. It is the author's view trending of this data offers an immediate early warning of major changes in the alignment state and steady state conditions of the machinery.

6.12 CONCLUSIONS

1) Most common machinery vibration problems can be diagnosed using discrete frequency analysis.

2) The effect of electromagnetic irregularity may be quantified by either speed or current analysis.

3) If a broken bar exists in a squirrel cage induction motor then this manifests itself as a 4 times RPM axial vibration component with a large modulation at twice slip frequency.

4) For maximum protection against catastrophic failure it is recommended that both the stator current and the change in axial vibration be monitored.

5) Since sidebands are to be investigated around the 1 and 2 times running speed zoom analysis must be available to detect these sidebands.

6) Vibration monitoring is a very useful tool in detecting a propagating transverse crack in a rotor shaft.

7) When monitoring vibration signals from transducers, it is important to distinguish between changes cuased by a crack and changes due to normal variations in parameters which influence the vibrations.

8) It is important to consider vector changes of vibration and not only changes in amplitude which could be considerably smaller due to phase shift.

9) Oil whip, oil whirl and rub can be readily diagnosed using shaft orbits or frequency spectrums from proximity probes.

10) Cascade or waterfall plots can also indicate the presence of oil whip and oil whirl.

11) The frequency spectrum for a bearing where oil whirl is present contains a sub-synchronous unstable frequency component at between 42-48% of the running speed.

12) Oil whirl and whip can be eliminated or reduced by changing certain bearing and rotor parameters.

13) Roller bearing defects can also be detected using discrete frequency analysis.

14) Trending of the shaft centre line position offers an immediate early warning of major changes in the alignment state of the machinery.

7. MODULE 4

DETERMINATION OF SHAFT CRITICAL SPEEDS USING COMPUTOR PREDICTIONS AND EXPERIMENTAL MEASUREMENTS

7.1 INTRODUCTION

As a result of a continuing demand for increased performance, many modern machines in the power generation service are designed to operate at shaft speeds approaching the first or second critical speed.

ESCOM requires that the operating speeds be at least twenty percent away from any critical speed. For draught group fans where blade passing frequencies are important the requirement is that no shaft critical must exist within 15% of the blade passing frequency.

Critical speeds are shaft speeds which coincide with the natural frequencies of the rotor bearing system. In most real machines, the natural frequencies are speed dependent since gyroscopic moments, fluid-film bearing stiffness, and fluid seal stiffness are all speed dependent.

A variety of methods can be employed to measure the critical speeds of a rotor bearing system. Some of these methods are:

1) Hammer impact test.
2) Shaft excitation method.
3) Transient synchronous vibration data from a vibration transducer during a coastdown or run-up.

The choice of method is usually constrained by practical or economic considerations when the measurement is to be made on an operational industrial machine.

The most widely used method for measuring critical speeds is done during a start-up or coastdown. The vibration signal from any suitable transducer can be fed through a synchronous tracking filter allowing a plot of synchronous vibration and phase as a function of running speed. The critical speeds are then identified by the peaks and a phase change on the Bodē plot. This method is usually the most practical and economical and was hence chosen.

Transient vibration data from two horizontally mounted accelerometers and a keyphasor pulse were recorded during a coastdown of four PA fans and two FD fans. The PA rotors were suspended in Cooper roller bearings and the FD rotors were suspended in fluid film bearings. Detailed analysis was performed on one PA fan, namely 2C, to demonstrate the various techniques to ascertain shaft critical speeds. These techniques include cascade plots, Nyquist plots and three dimensional Bodē Plots.

Computer programmes were developed to predict shaft critical speeds using the original Prohl matrix method and the transfer matrix method. The Prohl method uses an iterative process to satisfy the end boundary conditions. Using the transfer matrix method the boundary conditions are initially satisfied and an iterative process is employed to satisfy the end n^{th} degree polynomial depending on the number of sections comprising the shaft model.

Gyroscopic and rotational effects were included in the computer prediction of the shaft critical speeds. The effect of varying the bearing stiffness, on the predicted shaft critical speeds, was also investigated.

7.2 THEORY

The Bently Nevada ADRE system was used to process the transient data from the two accelerometers and the proximity probe. Two times RPM Bode plots were generated to determine the first shaft critical speed of the PA and FD impeller shafts. The two times RPM filtered component was used because the first shaft critical speed is above the operating speed for both the PA and FD fans investigatied. When the filtered second harmonic reaches the first shaft critical speed this results in maximum vibration amplitude and a phase change provided the system is not heavily-damped.

Only the first shaft critical speed was identified using this method. The digital vector filter of the ADRE system can only track and filter vibration components at half, one and two times the rate of the keyphasor pulse. In other words if a one-pulse-per-revolution keyphasor is present then the digital vector filter can filter the vibration components occurring at half, one and two times the operating speed. If a two-pulse-per-revolution keyphasor is present then the digital vector filter can filter the vibration components occurring at one, two and four times the operating speed. Analysing the filtered fourth harmonic will reveal the second shaft critical speed provided this occurs at a frequency which is below four times and greater than twice the operating speed. If the system is heavily-damped, the identification of the second, third and fourth shaft critical speeds from transient data is very difficult.

To illustrate how the first and second critical speeds can be identified from a Bodé and Nyquist plot a rundown from an alternator rotor that was balanced in the 300 tonne balancing pit at Rosherville will be examined. Figure 7.1 shows the

CAMDEN ALTERNATOR ROTOR.

HARMONIC 1 in micrometer peak peak
A.D.B. Absolute Displacements Bearing
MAXIMUM SCALE VALUE = 100.

FIGURE 7.1

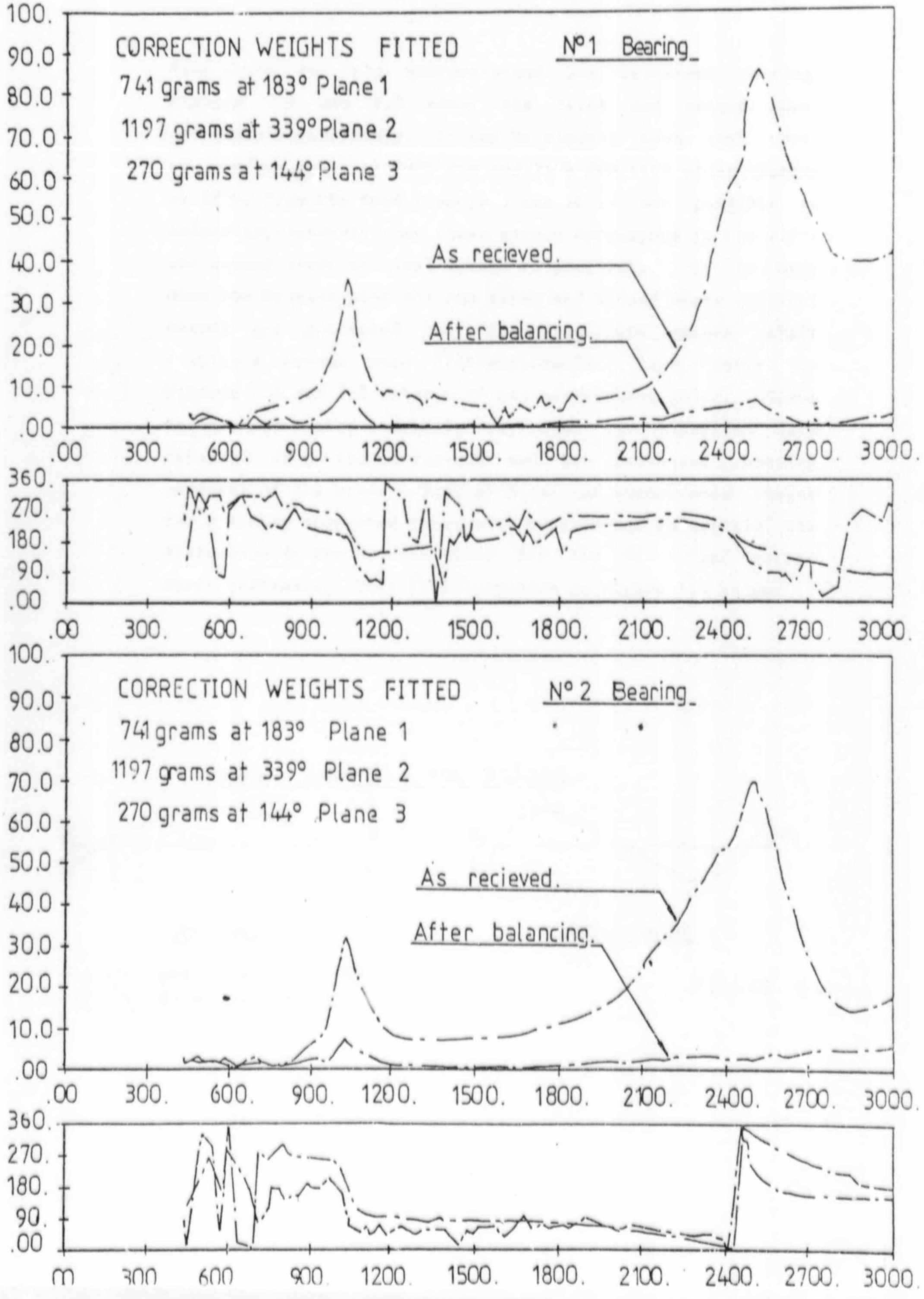

Bodē plots for the non-drive-end and drive-end bearing. Figures 7.2 and 7.3 shows the first and second shaft criticals respectively. It can be clearly seen that there are maximum peaks at 1005 RPM and 2499 RPM with phase changes of 180°. From the Bodē diagram alone it is not possible to deduce conclusively that these speeds correspond to the first and second shaft critical speeds respectively. It is only when the Nyquist plot for the first and second shaft critical speeds are generated that the first and second shaft criticals become more distinguishable. Each curve in Figures 7.2 and 7.3 relates to one measurement point. These measurement points normally represent the vibration data obtained from the drive-end and non drive-end bearing pedestal of the rotor. Typical first and second mode shapes for a simply supported rotor must be examined to explain the difference in the Nyquist plots for the first and second shaft criticals. This is illustrated in Figure 7.4 below.

MODE SHAPES FOR ROTORS

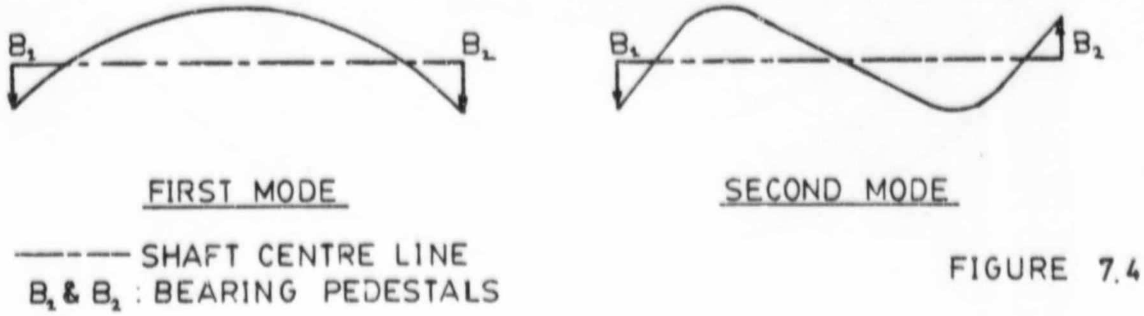

FIGURE 7.4

CAMDEN POWER STATION

ALTERNATOR ROTOR

Absolute Displacement Bearing

Amplitude μm peak–peak   Maximum scale = 40 μm

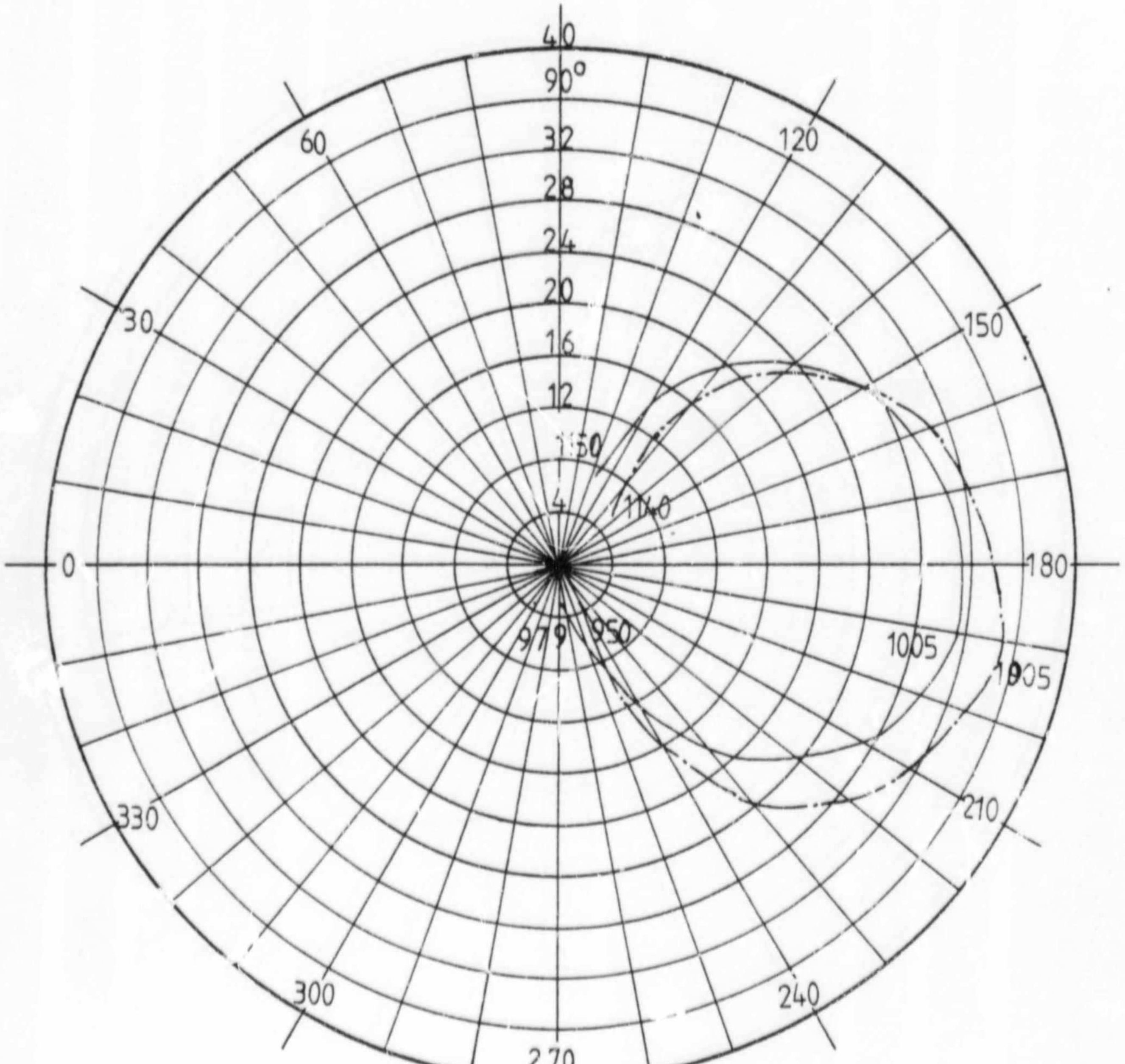

1st CRITICAL

—— Nº 1 BEARING
-·-·- Nº 2 BEARING

FIGURE 7.2

CAMDEN POWER STATION

ALTERNATOR ROTOR

Absolute Displacement Bearing

Amplitude μm peak—peak

Maximum scale = 100μm

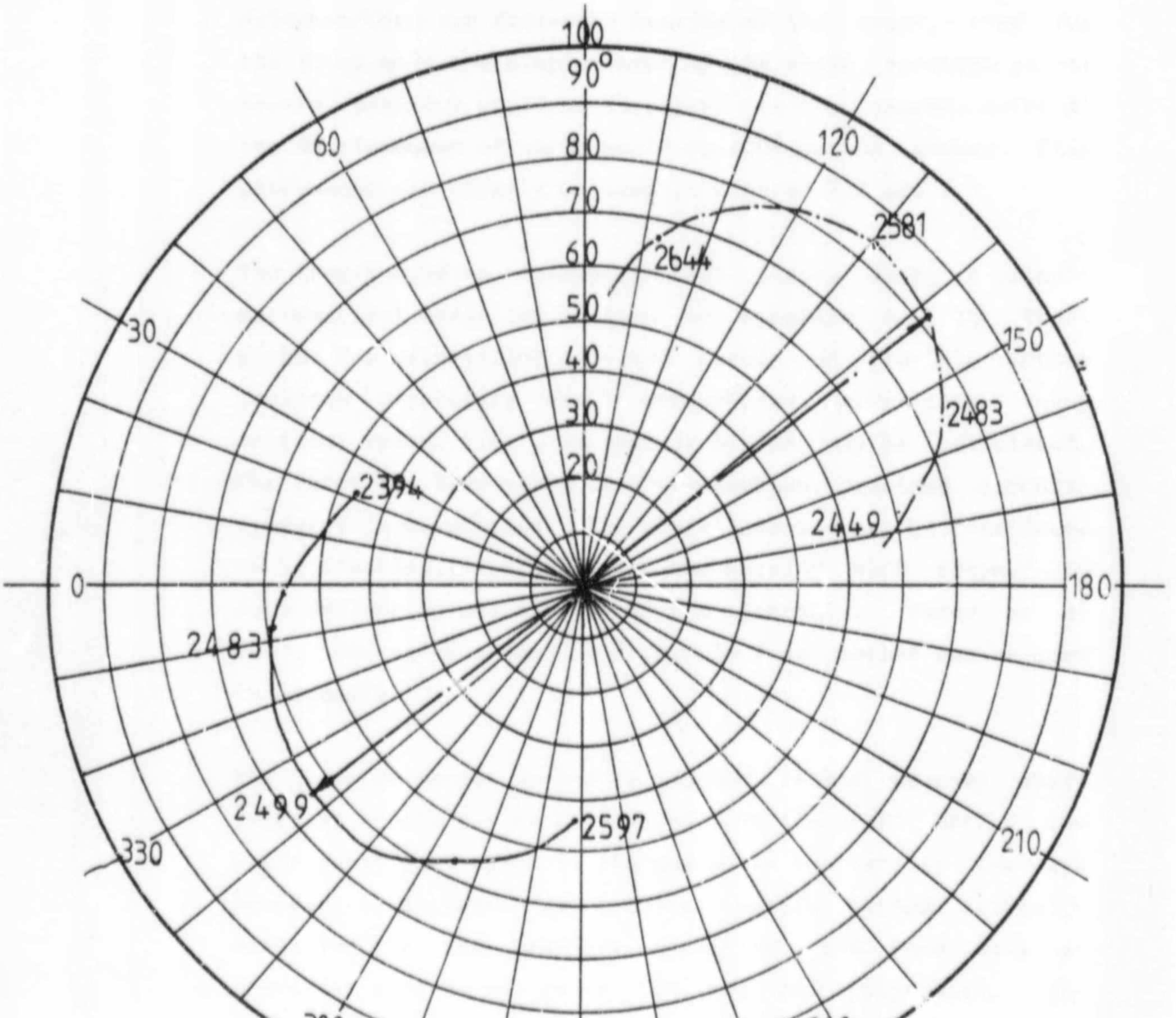

2nd CRITICAL

——— Nº 1 BEARING
- - - Nº 2 BEARING

FIGURE 7.3

From the mode shapes it is evident that if both transducers were mounted either vertically or horizontally at the drive-end and non drive-end bearing of the rotor, then for the first mode the displacement of the shaft, relative to its neutral position would be in phase. At the second critical the displacement of shaft would be 180^{o} out of phase. This phenomenon can clearly be seen in Figures 7.2 and 7.3.

The theory used to interpret Bodē plotes using a simple mathematical model can be seen in Appendix 4. The Prohl method for calculating critical speeds of flexible rotors combines generality with comparitive simplicity. Any critical speed, first, second, or higher, may be calculated. The rotor may have variable cross-section, provided circular symmetry is maintained. The shaft journals may be considered to be elastically supported in the bearing with respect to both deflection and fitting of the journals. Vance et el (44). The calculations used for the Prohl method can be seen in Appendix 5.

The transfer matrix method is another method whereby shaft critical speeds can be calculated. In the Prohl method the shaft rotational speed is changed so as to satisfy the end boundary conditions. The transfer matrix method initially satisfies the end boundary conditions and then uses an iterative process to solve for the end polynomial. The calculations used for this method can be seen in Appendix 6.

7.3 OBJECTIVES

1) To determine the accuracy and reliability of various computer prediction programmes used to calculate shaft critical speeds by comparing them with experimental measurements obtained during a coastdown of four PA and two FD fans.
2) To determine the effect of excluding gyroscopic and inertia effects on the predicted shaft critical speeds.
3) To determine the effect of changing the bearing stiffness on the predicted shaft critical speeds.
4) To obtain mode shapes for the PA and FD fan rotors.
5) To develop computer software to predict shaft critical speeds.

7.4 APPARATUS

7.4.1 Experimental Measurements

Recorders

TEAC seven channel tape recorder with built in amplifiers, type MR-30.

Transducers

Two B&K accelerometers type 4371
One Bently Nevada proximity probe, series 7200

Filters

Wavetek 24D tracking filter

Analysers

Wavetek 100A FFT analyser
Bently Nevada ADRE system

Amplifiers

Two B&K charge amplifiers type 2685
One Bently Nevada amplifier type 29191

Power Supply

One -24V DC Bently Nevada power supply type 44120-01

Oscillator/Demodulator

One Bently Nevada oscillator/demodulator series 7200

7.4.2 Computer Predictions

Hewlett Packard 9836 desk top computer
Hewlett Packard printer
Olivetti M24 personal computer

7.4.3 Details of Fan Impellers

PA	Impeller rotor		
	Impeller mass	=	1030 kg
	Rotor and impeller mass	=	1340 kg
	Young´s Modulus	=	206,0 MPa
	Material density	=	7833,0 kg/m^3
	Design speed	=	1490 RPM
FD	Impeller rotor		
	Impeller mass	=	8310 kg
	Rotor and impeller mass	=	22 679,0 kg
	Coupling mass	=	277,10 kg
	Young´s Modulus	=	206,0 MPa
	Material density	=	7833,0 kg/m^3
	Design speed	=	740 RPM

See Figure 7.5 for overall dimensions of the PA and FD fan rotor.

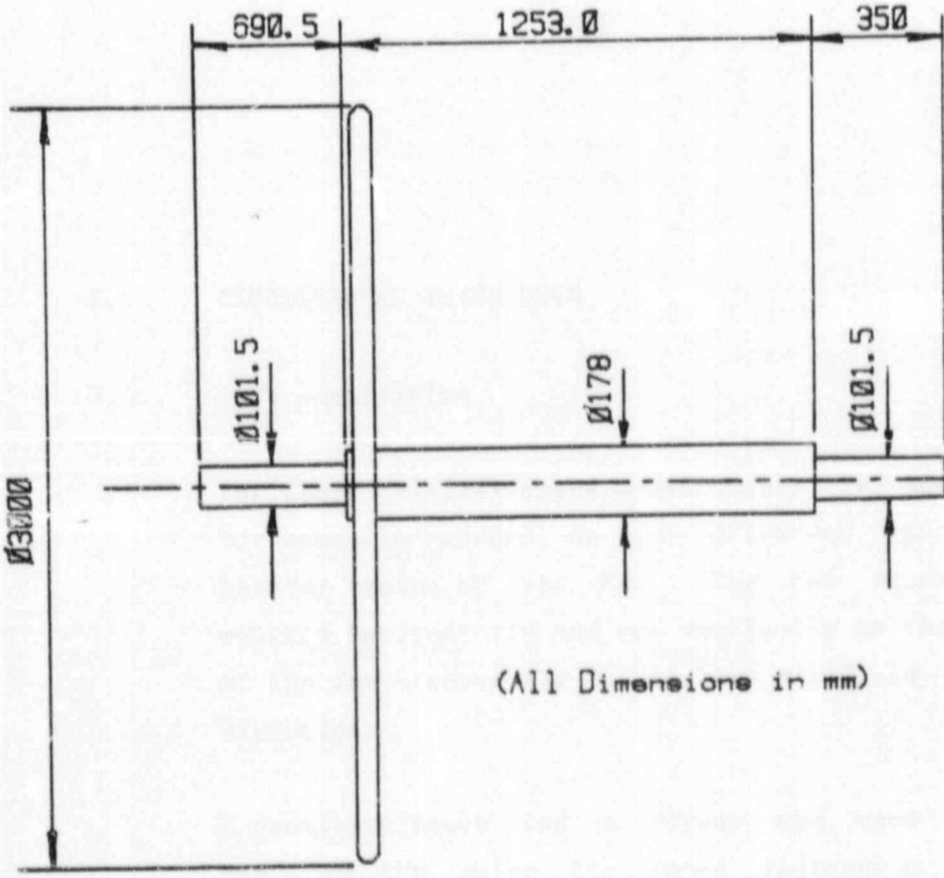

OVERALL DIMENSIONS FOR PA FAN ROTOR

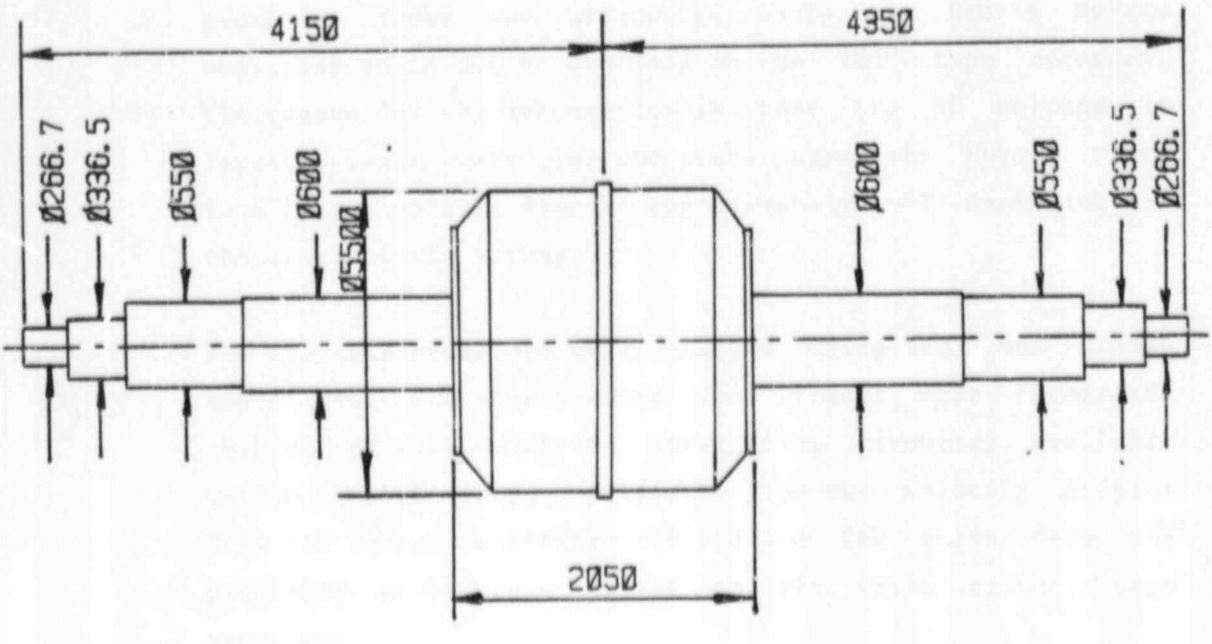

OVERALL DIMENSIONS FOR FD FAN ROTOR.

FIGURE 7.5

7.5 EXPERIMENTAL TECHNIQUES

7.5.1 Data Acquisition

For shaft critical speed measurements, an accelerometer was horizontally mounted on the drive-end and non drive-end bearing casing of the fan. The two accelerometers were mounted horizontally and not vertically on the bearing casing of the fan because the fan is less stiff in the horizontal direction.

A proximity probe and a keyway was used to generate a one-times-RPM pulse for speed indication and tracking purposes. The DC and AC voltages from the proximity probe were filtered in such a way that only the AC voltage remained, with the DC voltage supressed. This was achieved using the Bently Nevada amplifier. The AC voltage from the proximity probe was attenuated using the Bently Nevada amplifier so as not to overload on the TEAC tape recorder. The reason for the attenuation is that the AC voltage is large, because every time the probe passes the keyway there is a larger voltage drop of approximately -8V depending on the depth of the keyway. .

The two accelerometers were charged using the B&K charge amplifiers. The acceleration time traces were integrated once to velocity using the integrating circuitry available within the B&K charge amplifiers. The two velocity outputs from the charge amplifiers and the 1 x RFM pulse from the proximity probe were stored on the seven channel tape recorder.

The Wavetek 100A FFT analyser was used to ascertain if the outputs, from the two accelerometers and the proximity probe, were in any way spurious. The Wavetek 24D tracking filter was used as a speed indicator. Speed indication is important for run-ups and coastdowns as it indicates when to stop and commence the recording of the data, and for the generation of Bodé and Nyquist plots. Figure 7.6 shows the general layout of the equipment and instrumentation.

7.5.2 Data Analysis

The determination of the experimental shaft criticals involved the generation of synchronised Bodé and Nyquist plots using the ADRE system. The system configuration of the ADRE system can be seen in Figure 7.7. The physical configuration of the ADRE system can be seen in Figure 7.8.

The two velocity signals and the pulse from the proximity probe, stored on the tape, were fed into the Digital Vector filter of the ADRE system. One, and two times filtered RPM Bodé, and Nyquist plots were generated using the ADRE software.

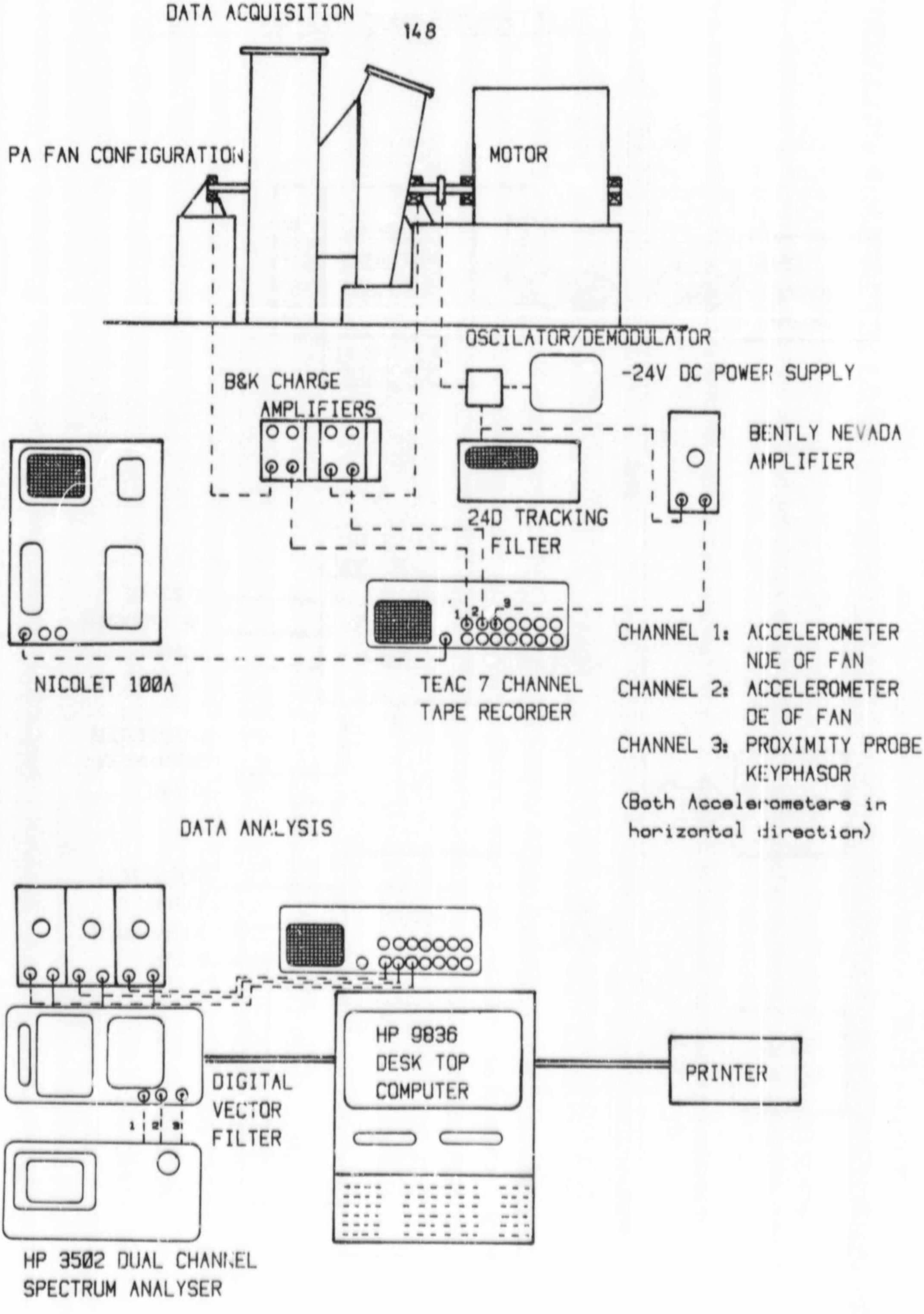

GENERAL LAYOUT OF EQUIPMENT AND INSTRUMENTATION

FIGURE 7.6

ADRE SYSTEM CONFIGURATION

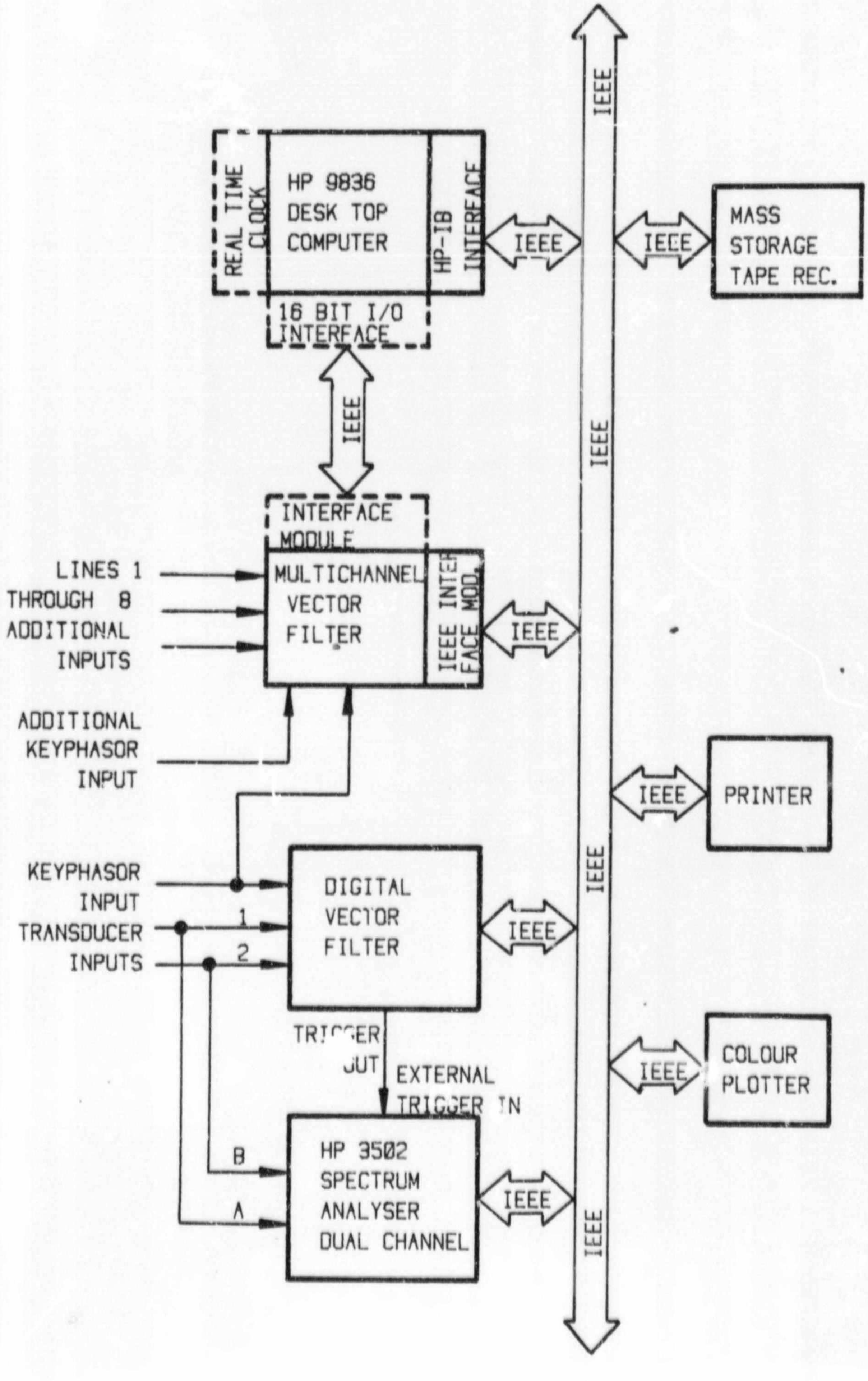

FIGURE 7.7

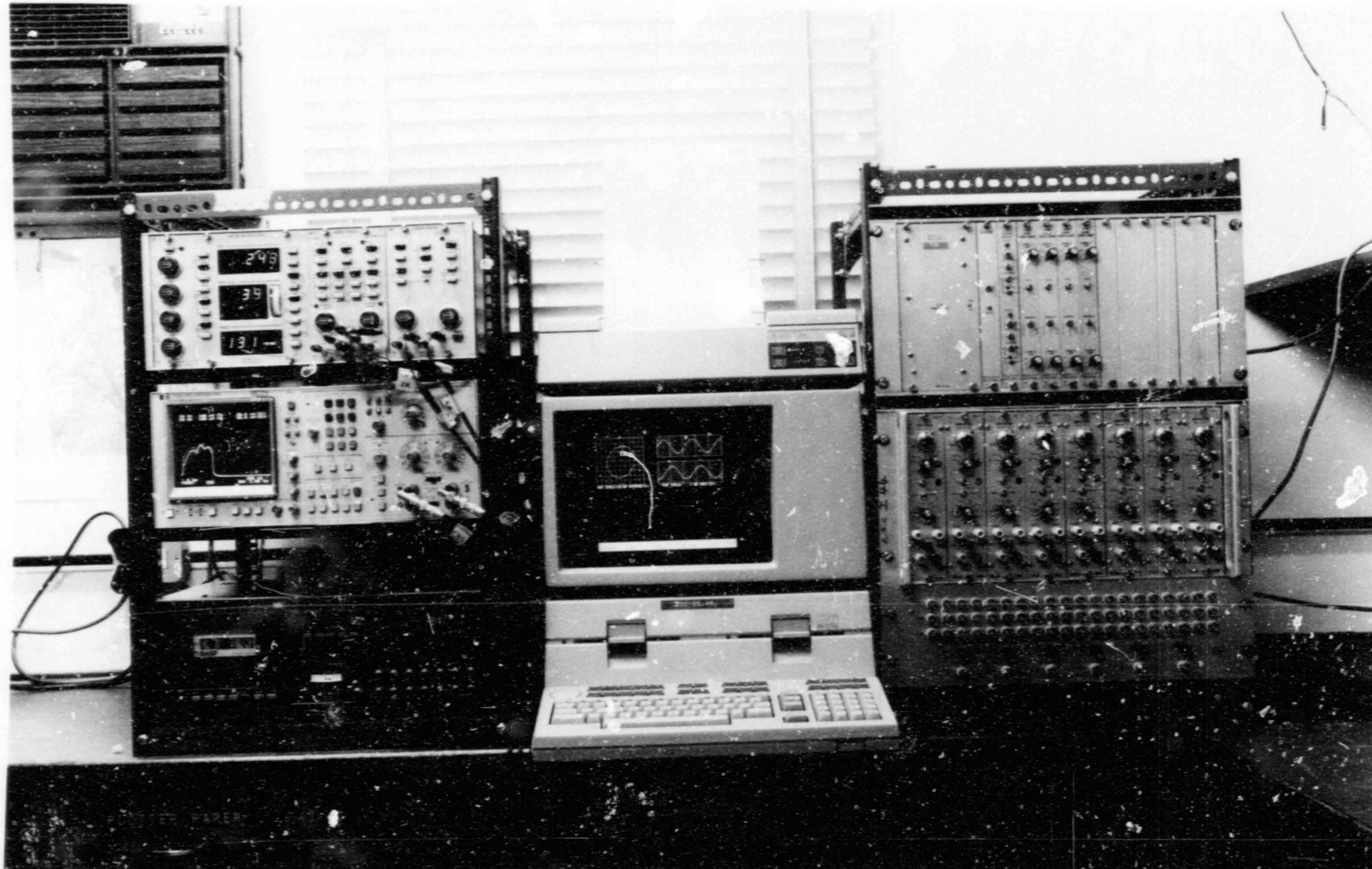

AUTOMATED DIAGNOSTICS FOR ROTATING EQUIPMENT (ADRE) SYSTEM FIGURE 7.8

7.5.3 Technique used for the Computer Prediction

The technique used for the calculation of the predicted shaft criticals used the following steps in chronological order.

1) Divide each constant diameter section into numerous sections of length approximately 50 mm.

2) Calculate the mass of each of these sections of length approximately 50 mm.

3) Assume the impeller mass to be an evenly distributed mass along the length of the shaft where the impeller is attached to the shaft.

4) Divide the total impeller mass by the number of $\pm$ 50 mm sections it spans.

5) Calculate the mass of the two end overhanging shafts that are not between the bearing centres. These two masses are added to the first and last sections' equivalent masses.

6) Construct the idealised system so that the total mass within a given section is divided into two parts which are concentrated at the ends of the section, this division of mass being such that the centre of gravity of the section mass remains unchanged.

7) For the calculation of the gyroscopic constants A and B, the distributed impeller mass at each section was considered as a thin disk of equivalent mass, having a specified diameter and a calcuated thickness h. See Appendix 7.